# Projection-based Iterative Learning Control for Ball-screw-driven Stage Using Basis Function and Data-based Friction Model

Takumi HAYASHI, Hiroshi FUJIMOTO
*The University of Tokyo*
5-1-5, Kashiwanoha, Kashiwa, Chiba, 277-8561, Japan
hayashi.takumi18@ae.k.u-tokyo.ac.jp, fujimoto@k.u-tokyo.ac.jp

Yoshihiro ISAOKA, Yuki TERADA
*DMG MORI CO., LTD.*
362, Idono, Yamatokoriyama, Nara, 639-1183 Japan
yo-isaoka@dmgmori.co.jp, yk-terada@dmgmori.co.jp

***Abstract*—This paper presents precise control of ball-screw-driven stages based on projection-based iterative learning control (ILC). Standard ILC has a problem that only one reference trajectory can be learned and once the reference trajectory is changed to other, relearning is required. To overcome this problem, projection-based ILC using basis functions has been studied. To apply projection-based ILC to position control of ball-screw-driven stages, a model of rolling friction is needed. An approximation of rolling friction is introduced in the previous study, but this deteriorates control performance. In this paper, therefore, projection-based ILC using basis functions and data-based friction model which needs no approximation is proposed. Simulations and experiments verify the effectiveness of our proposal.**

***Index Terms*—Iterative learning control, projection-based iterative learning control, ball-screw-driven stage, rolling friction compensation, data-based friction model.**

## I. Introduction

Iterative learning control (ILC) [1] is an effective feedforward control method when the same reference trajectory (task) is repeated in all trials and disturbance is trial-invariant. In ILC, feedforward input is updated in every trial to improve control performance by learning the tracking error of the previous trial. Even though modeling error and trial-invariant disturbance exist, control performance can be improved gradually and owing to this feature, ILC is attracting more and more attention [2]. However, ILC has a vulnerability to reference trajectory variation. ILC is effective under the assumption that the reference trajectory and disturbance are common to each trial. Once this assumption is violated, ILC cannot improve control performance. To overcome this problem, ILC using basis functions have been studied [3], [4]. This type of ILC is called projection-based ILC.

In this paper, an application of projection-based ILC to position control of ball-screw-driven stages is considered. Ball-screw-driven stages, shown in Fig. 1, are feed systems which convert motor's rotational motion into stage's translational motion. They are widely used in industrial equipment such as numerically controlled (NC) machine tools. Therefore, precise position control of ball-screw-driven stages is needed. However, friction, which is called rolling friction, occurs

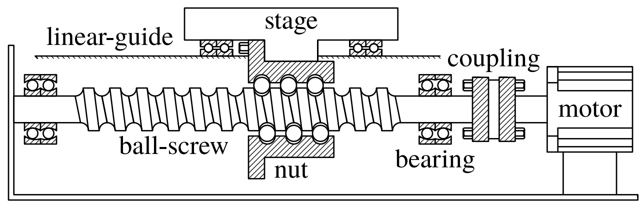


Fig. 1: Overview of a ball-screw-driven stage.

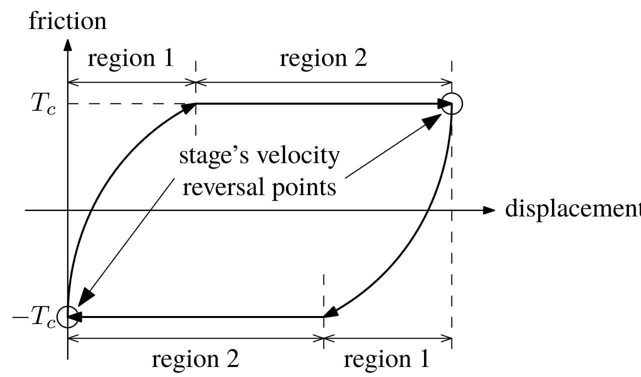


Fig. 2: Characteristic of rolling friction of ball-screw-driven stages.

on ball-screw and linear-guide and this friction deteriorates control performance. As shown in Fig. 2, rolling friction has a dependency on displacement from the stage's velocity reversal point. In region 1 in Fig. 2, nonlinear elastic characteristic exists. In region 2, rolling friction shows Coulomb friction $T_c$ which is almost constant. Because of this friction, it is well known that large error arises when the stage's velocity reverses.

Rolling friction compensation is needed for precise control. In many studies, rolling friction is measured precisely by ultra-low speed examination and friction models are designed based on measured data [5]–[7]. Rolling friction can be compensated if the friction model is designed well. However, rolling friction depends on environments and operating conditions [8]. If its characteristic changes from measurement time, rolling friction

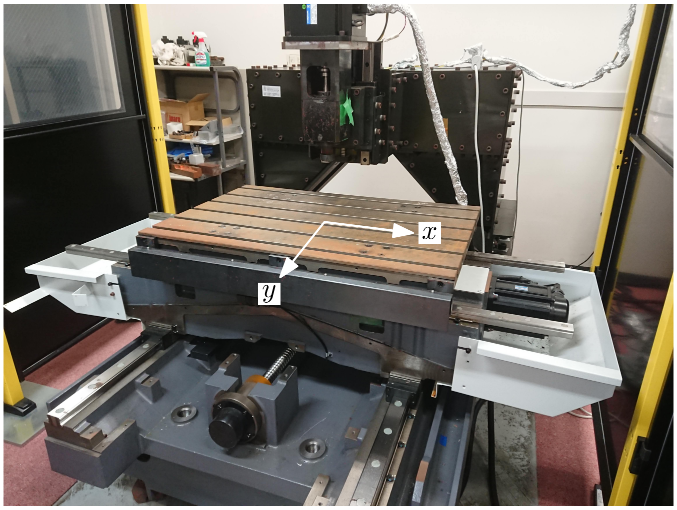


Fig. 3: Picture of the experimental setup. Only the $x$ axis is used in this paper.

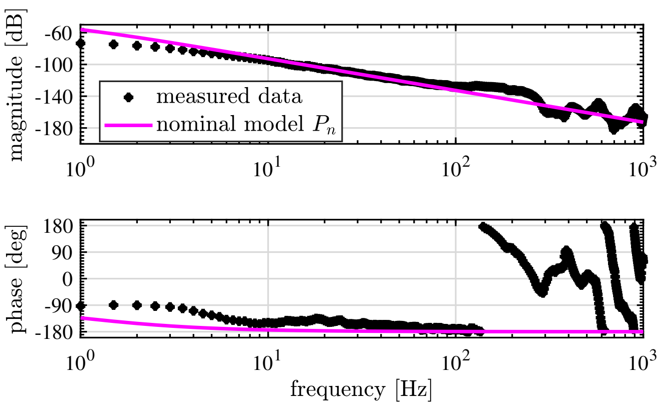


Fig. 4: Frequency response from motor's current $i$ [A] to stage's position $x$ [m] of the $x$-axis of the experimental setup shown in Fig. 3.

cannot be compensated.

This paper, therefore, considers the other approach, learning-based friction compensation [9]. Projection-based ILC is adopted to compensate rolling friction. To consider rolling friction compensation in projection-based ILC, rolling friction is approximated in the previous study [10]. However, this approximation deteriorates control performance. Therefore, to suppress tracking error, projection-based ILC using basis functions and data-based friction model [11] which requires no equation model of rolling friction is proposed in this paper. Our proposal is verified through simulations and experiments.

## II. Experimental Setup

### A. Model of Experimental Setup

Fig. 3 shows our experimental setup. Our experimental setup has two axes. In this paper, only the $x$ axis is used. According to frequency response data from motor's current $i$ [A] to stage's position $x$ [m] shown in Fig. 4, nominal model of our experimental setup is obtained as

$$P_n(s) = \frac{RK_T}{J_n s^2 + D_n s}. \tag{1}$$

Table I shows the meaning and value of each parameter.

TABLE I: Parameters of the experimental setup.

| | |
|---|---|
| Nominal inertia $J_n$ | $0.015\,\mathrm{kgm^2}$ |
| Nominal viscosity coefficient $D_n$ | $0.1\,\mathrm{N\,m\,s\,rad^{-1}}$ |
| Torque constant $K_T$ | $0.715\,\mathrm{N\,m\,A^{-1}}$ |
| Ball-screw's lead $R$ | $1.91\,\mathrm{mm\,rad^{-1}}$ |

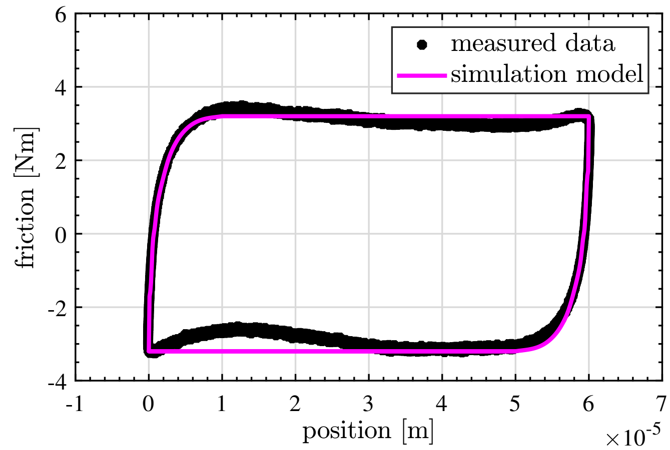


Fig. 5: Rolling friction of the experimental setup. Black points are data measured by ultra-low speed examination and magenta line denotes simulation model. Note that this simulation model is only used in simulation.

### B. Rolling Friction of Experimental Setup

Rolling friction of our experimental setup measured by ultra-low speed examination is shown in Fig. 5. According to this data, the width of region 1 in Fig. 2 and Coulomb friction $T_c$ are estimated to be about $10\,\mu\mathrm{m}$ and $3.2\,\mathrm{N\,m}$, respectively.

## III. Iterative Learning Control

### A. Standard ILC

*1) Feedforward Input Update Law:* Two-degree-of-freedom control system shown in Fig. 6 is considered. Tracking error $e$ is calculated as

$$e = r - x = Sr - SP(f - d). \tag{2}$$

Here, $S = (1 + C_{\mathrm{FB}}P)^{-1}$ is a sensitivity function.

In ILC, the same reference trajectory is repeated in all trials and disturbance is trial-invariant. In this situation, by using the $j$th trial's feedforward input $f_j$ and the tracking error $e_j$, the next trial's feedforward input $f_{j+1}$ is calculated as follows:

$$f_{j+1} = Q(f_j + Le_j). \tag{3}$$

$L$ and $Q$ are called learning filter and robust filter, respectively. In this paper, values with subscript $j$ and $j+1$ denote values of the $j$th and $j+1$th trial of ILC, respectively.

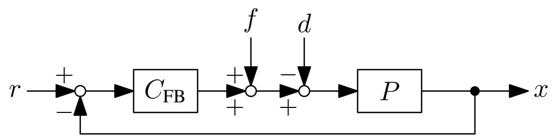


Fig. 6: Block diagram of two-degree-of-freedom control system. Here, $r$, $x$, $f$, and $d$ denote (position) reference, (position) output, feedforward input, and disturbance, respectively. $P$ and $C_{\mathrm{FB}}$ denote a plant (linear time-invariant system) and a feedback controller, respectively. In this paper, $d$ is rolling friction and $P$ is a ball-screw-driven stage.

*2) Tracking Error Convergence:* From (2), the $j$th and $j+1$th trial's tracking error $e_j$, $e_{j+1}$ are expressed as follows:

$$e_j = Sr_j - SP(f_j - d_j), \tag{4}$$

$$e_{j+1} = Sr_j - SP(f_{j+1} - d_j). \tag{5}$$

Under the assumption that reference $r$ and disturbance $d$ is the same in all trials (*i.e.*, $r_j = r_{j+1} = r$, $d_j = d_{j+1} = d$), a recurrence relation (6) can be obtaind from (3), (4), and (5).

$$e_{j+1} = Q(1 - SPL)e_j + (1 - Q)(Sr - SPd). \tag{6}$$

Therefore, the tracking error is monotonically decreases if (7) is satisfied.

$$\max_{\omega} \left| Q\left(\mathrm{e}^{\mathrm{j}\omega}\right)\left(1 - S\left(\mathrm{e}^{\mathrm{j}\omega}\right)L\left(\mathrm{e}^{\mathrm{j}\omega}\right)P\left(\mathrm{e}^{\mathrm{j}\omega}\right)\right)\right| < 1. \tag{7}$$

In this paper, $L$ and $Q$ are designed based on frequency-domain information [1].

### *B. Projection-based Iterative Learning Control Using Basis Functions*

A serious problem of standard ILC is that once learned reference trajectory is changed to other, relearning is needed. To overcome this problem, projection-based ILC has been studied. In projection-based ILC, basis functions are introduced. By parameterizing feedforward input by using basis functions, the plant's parameters are estimated in each trial and tolerance to reference trajectory variation can be obtained.

When a plant is represented as

$$P(s) = \frac{RK_T}{Js^2 + Ds}, \tag{8}$$

feedforward input which can suppress tracking error in continuous time is expressed as (9) if disturbance is ignored.

$$\begin{aligned} f &= \frac{J}{RK_T}\ddot{r} + \frac{D}{RK_T}\dot{r} \\ &= \begin{bmatrix} \ddot{r} & \dot{r} \end{bmatrix} \begin{bmatrix} \frac{J}{RK_T} \\ \frac{D}{RK_T} \end{bmatrix}. \end{aligned} \tag{9}$$

In projection-based ILC, parameterized feedforward input $\boldsymbol{f}^{\mathrm{p}}$ is calculated by using basis functions $\boldsymbol{\Psi}(\boldsymbol{r})$ and plant's parameters $\boldsymbol{\theta}$ as follows:

$$\boldsymbol{f}^{\mathrm{p}} = \boldsymbol{\Psi}(\boldsymbol{r})\boldsymbol{\theta}, \tag{10}$$

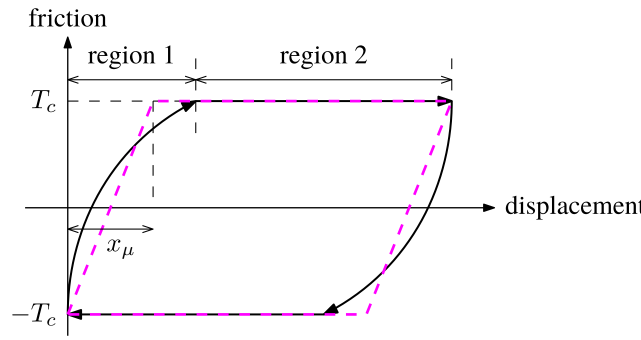


Fig. 7: Real characteristics (black solid line) and approximation model (magenta dashed line) of rolling friction .

where $\boldsymbol{\Psi}(\boldsymbol{r}) \in \mathbb{R}^{(N+1)\times n_\theta}$ and $\boldsymbol{\theta} \in \mathbb{R}^{n_\theta}$. $\boldsymbol{r}$ is a reference trajectory （*i.e.*, $\boldsymbol{r} = [r[0]\ r[1]\ \cdots\ r[N]]^\top$, $r[i] = r(iT_s)$, $N$: length of one trial of ILC, $T_s$: sampling time）. $n_\theta$ is the number of the plant's parameters.

To obtain robustness to reference trajectory variation, the plant's parameter estimation is a key issue and projection-based ILC consists three steps [3].

1) Assume that the current trial's reference trajectory $\boldsymbol{r}_j$ is repeated in the next trial, and calculate the next trial's feedforward input $\boldsymbol{f}^{\mathrm{np}}_{j+1}$ by (3).
2) Estimate the plant's parameters $\boldsymbol{\theta}_{j+1}$ by using $\boldsymbol{f}^{\mathrm{np}}_{j+1}$ and $\boldsymbol{\Psi}(\boldsymbol{r}_j)$.
3) Update $\boldsymbol{r}_j \rightarrow \boldsymbol{r}_{j+1}$ and $\boldsymbol{\Psi}(\boldsymbol{r}_j) \rightarrow \boldsymbol{\Psi}(\boldsymbol{r}_{j+1})$. Then, calculate the feedforward input $\boldsymbol{f}^{\mathrm{p}}_{j+1}$ by using $\boldsymbol{\Psi}(\boldsymbol{r}_{j+1})$ and $\boldsymbol{\theta}_{j+1}$ as follows:

$$\boldsymbol{f}^{\mathrm{p}}_{j+1} = \boldsymbol{\Psi}(\boldsymbol{r}_{j+1})\boldsymbol{\theta}_{j+1}. \tag{11}$$

*1) Choice of Basis Functions and Plant's Parameters:* To achieve precise control of ball-screw-driven stages, rolling friction must be compensated. To compensate rolling friction by projection-based ILC, its approximation is introduced [10]. Rolling friction whose real characteristics are shown as the black solid line in Fig. 7 is approximated as the magenta dashed line in Fig. 7. Owing to this approximation, rolling friction $T_{\mathrm{rf}} = d$ can be parameterized as follows:

$$\begin{aligned} T_{\mathrm{rf}} &\approx \mathrm{sign}(\dot{x}(t)) \cdot \min\left(\frac{2T_c}{x_\mu}x_r - T_c,\, T_c\right)/K_T \\ &= \frac{T_c}{K_T} \cdot \mathrm{sign}(\dot{x}(t)) \min\left(\frac{2}{x_\mu}x_r - 1,\, 1\right) \\ &= \frac{T_c}{K_T} \cdot b_{\mathrm{rf}}(t), \end{aligned} \tag{12}$$

where

$$b_{\mathrm{rf}}(t) = \mathrm{sign}(\dot{x}(t)) \min\left(\frac{2}{x_\mu}x_r - 1,\, 1\right). \tag{13}$$

$x_\mu$ is a tuning parameter which has a role to compensate nonlinear elastic characteristic of rolling friction. $x_r$ denotes displacement from stage's velocity reversal point. In (12), rolling friction is divided by torque constant $K_T$ to convert its unit from [Nm] to [A].

According to (9) and (12), basis functions $\boldsymbol{\Psi}(\boldsymbol{r})$ and plant's parameters $\boldsymbol{\theta}$ are given by (14a) and (14b), respectively. Note that $b_{\mathrm{rf}}[i] = b_{\mathrm{rf}}(iT_s)$ is calculated based on reference trajectory $\boldsymbol{r}$.

$$\boldsymbol{\Psi}(\boldsymbol{r}) = \begin{bmatrix} \ddot{r}[0] & \dot{r}[0] & b_{\mathrm{rf}}[0] \\ \ddot{r}[1] & \dot{r}[1] & b_{\mathrm{rf}}[1] \\ \vdots & \vdots & \vdots \\ \ddot{r}[N] & \dot{r}[N] & b_{\mathrm{rf}}[N] \end{bmatrix}, \tag{14a}$$

$$\boldsymbol{\theta} = \begin{bmatrix} \frac{J}{RK_T} & \frac{D}{RK_T} & \frac{T_c}{K_T} \end{bmatrix}^{\top}. \tag{14b}$$

*2) Plant's Parameter Estimation:* Plant's parameters are estimated by using predicted tracking error [3]. According to (2), $j$th trial's tracking error $\boldsymbol{e}_j$ is expressed as (15) using lifted system representation.

$$\boldsymbol{e}_j = \mathcal{S}\boldsymbol{r}_j - \mathcal{S}\mathcal{P}(\boldsymbol{f}_j - \boldsymbol{d}_j), \tag{15}$$

where $\mathcal{P}$ and $\mathcal{S}$ are convolution matrices of $P$ and $S$, respectively. In the same way as (15), when $\boldsymbol{f}^{\mathrm{np}}_{j+1}$ is applied as feedforward input under the condition that reference is $\boldsymbol{r}_j$ and disturbance is $\boldsymbol{d}_j$, tracking error $\boldsymbol{e}^{\mathrm{np}}_j$ is expressed as follows:

$$\boldsymbol{e}^{\mathrm{np}}_j = \mathcal{S}\boldsymbol{r}_j - \mathcal{S}\mathcal{P}\big(\boldsymbol{f}^{\mathrm{np}}_{j+1} - \boldsymbol{d}_j\big). \tag{16}$$

Therefore, $\boldsymbol{e}^{\mathrm{np}}_j$ can be predicted as $\hat{\boldsymbol{e}}^{\mathrm{np}}_j$ by (15) and (16) using nominal model.

$$\hat{\boldsymbol{e}}^{\mathrm{np}}_j = \boldsymbol{e}_j - \mathcal{S}_n\mathcal{P}_n\big(\boldsymbol{f}^{\mathrm{np}}_{j+1} - \boldsymbol{f}_j\big). \tag{17}$$

Here, subscript $n$ denotes nominal model.

Furthermore, when $\boldsymbol{\Psi}(\boldsymbol{r}_j)\boldsymbol{\theta}_{j+1}$ is applied as feedforward input, tracking error can be also predicted as follows:

$$\hat{\boldsymbol{e}}^{\mathrm{p}}_j = \boldsymbol{e}_j - \mathcal{S}_n\mathcal{P}_n(\boldsymbol{\Psi}(\boldsymbol{r}_j)\boldsymbol{\theta}_{j+1} - \boldsymbol{f}_j). \tag{18}$$

According to [3], plant's parameters $\boldsymbol{\theta}_{j+1}$ are estimated by solving (19). This optimization problem can be solved by the least squares method.

$$\begin{aligned} &\min_{\boldsymbol{\theta}_{j+1}} \big|\big|\hat{\boldsymbol{e}}^{\mathrm{np}}_j - \hat{\boldsymbol{e}}^{\mathrm{p}}_j\big|\big|_2 \\ &\Rightarrow \min_{\boldsymbol{\theta}_{j+1}} \big|\big|\mathcal{S}_n\mathcal{P}_n\boldsymbol{f}^{\mathrm{np}}_{j+1} - \mathcal{S}_n\mathcal{P}_n\boldsymbol{\Psi}(\boldsymbol{r}_j)\boldsymbol{\theta}_{j+1}\big|\big|_2 \end{aligned} \tag{19}$$

### *C. Our Proposal – Basis Functions and Data-based Friction Model Approach*

In (19), the approximation model of rolling friction is used for parameterization. Due to this approximation, modeling error of rolling friction exists and this may deteriorate control performance. In this paper, to avoid modeling error of rolling friction, the data-based friction model [11] is introduced. Unlike the other rolling friction models, this model uses a friction table instead of equations. The friction table, as shown in Fig. 8, stores displacement from the stage's velocity reversal point and rolling friction to realize the nonlinear elastic characteristic of rolling friction. The proposed method consists following five steps.

1) Calculate $\boldsymbol{f}^{\mathrm{np}}_{j+1}$.
2) Estimate $\boldsymbol{\theta}_{j+1}$.

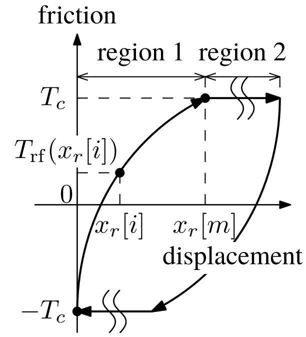


| displacement $x_r$ [m] | rolling friction $T_{\mathrm{rf}}(x_r)$ [Nm] |
|---|---|
| 0 | $-T_c$ |
| $\vdots$ | $\vdots$ |
| $x_r[i]$ | $T_{\mathrm{rf}}(x_r[i])$ |
| $\vdots$ | $\vdots$ |
| $x_r[m]$ | $T_c$ |

Fig. 8: Concept of friction table for data-based friction model. Nonlinear elastic characteristic of rolling friction (left) is represented as table (right) without any approximations.

3) Estimate the rolling friction $\hat{\boldsymbol{T}}_{\mathrm{rf},j+1}$ as follows:

$$\hat{\boldsymbol{T}}_{\mathrm{rf},j+1} = \left(\boldsymbol{f}^{\mathrm{np}}_{j+1} - \frac{\hat{J}_{j+1}}{RK_T}\ddot{\boldsymbol{r}}_j - \frac{\hat{D}_{j+1}}{RK_T}\dot{\boldsymbol{r}}_j\right)K_T, \tag{20}$$

where $\boldsymbol{\theta}_{j+1} = \begin{bmatrix} \frac{\hat{J}_{j+1}}{RK_T} & \frac{\hat{D}_{j+1}}{RK_T} & \frac{\hat{T}_{cj+1}}{K_T} \end{bmatrix}^{\top}$.

4) Obtain the friction table from $\boldsymbol{r}_j$ and $\hat{\boldsymbol{T}}_{\mathrm{rf},j+1}$ as Fig. 8.
5) Update $\boldsymbol{r}_j \rightarrow \boldsymbol{r}_{j+1}$ and $\boldsymbol{\Psi}(\boldsymbol{r}_j) \rightarrow \boldsymbol{\Psi}(\boldsymbol{r}_{j+1})$. Then, calculate the feedforward input $\boldsymbol{f}^{\mathrm{p}}_{j+1}$ by using $\boldsymbol{\Psi}(\boldsymbol{r}_{j+1})$, $\boldsymbol{\theta}_{j+1}$, and obtained friction table. When $\boldsymbol{r}_{j+1} \neq \boldsymbol{r}_j$, the closest value of the friction table is used for rolling friction compensation.

To make the friction table in each trial, the plant's parameters need to be estimated precisely because modeling error cannot be ignored in practical use speed [12]. In (19), the plant's parameters are estimated by using the approximation model of rolling friction, but this approximation may have a bad influence on the plant's parameter estimation. Therefore, another estimation method is proposed.

To eliminate the influence of rolling friction approximation in the plant's parameter estimation, a weighting matrix $\boldsymbol{W}_j$ is introduced. Then, instead of (19), another optimization problem (21) is solved to determine plant's parameters $\boldsymbol{\theta}_{j+1}$.

$$\min_{\boldsymbol{\theta}_{j+1}} \left|\left|\mathcal{S}_n\mathcal{P}_n\boldsymbol{f}^{\mathrm{np}}_{j+1} - \mathcal{S}_n\mathcal{P}_n\overline{\boldsymbol{f}}^{\mathrm{p}}_{j+1}(\boldsymbol{r}_j, \boldsymbol{W}_j)\right|\right|_2, \tag{21}$$

$$\overline{\boldsymbol{f}}^{\mathrm{p}}_{j+1}(\boldsymbol{r}_j, \boldsymbol{W}_j) = \boldsymbol{W}_j\boldsymbol{\Psi}(\boldsymbol{r}_j)\boldsymbol{\theta}_{j+1} + (\boldsymbol{I} - \boldsymbol{W}_j)\boldsymbol{f}^{\mathrm{np}}_{j+1}. \tag{22}$$

Equation (21) can be rewritten as (23) and (23) can be also solved by the least squares method.

$$\min_{\boldsymbol{\theta}_{j+1}} \big|\big|\mathcal{S}_n\mathcal{P}_n\boldsymbol{W}_j\boldsymbol{f}^{\mathrm{np}}_{j+1} - \mathcal{S}_n\mathcal{P}_n\boldsymbol{W}_j\boldsymbol{\Psi}(\boldsymbol{r}_j)\boldsymbol{\theta}_{j+1}\big|\big|_2 \tag{23}$$

The weighting matrix $\boldsymbol{W}_j$ is determined based on $\boldsymbol{r}_j$. By designing proper weighting matrix $\boldsymbol{W}_j$, the influence of nonlinear elastic characteristic of rolling friction can be suppressed in the estimation step and thus the plant's parameters can be estimated precisely. Design method of $\boldsymbol{W}_j$ is described in the next section.

## IV. SIMULATION

Simulations are conducted to verify effectiveness of our proposal. Through simulations, following three methods are compared.

- Standard ILC (S-ILC): Feedforward input is calculated as (3). No basis functions are used.
- Projection-based ILC using the basis functions (P-ILC (B.F.)): The plant's parameters are estimated by (19) and feedforward input is calculated as (11).
- Projection-based ILC using the basis functions and the data-based friction model (friction table) (P-ILC (B.F.+F.T.)): The plant's parameters are estimated by (23) and feedforward input is calculated using friction table. This method is our proposal.

The sampling time $T_s$ is set to $1\,\mathrm{ms}$.

### A. Conditions

*1) Simulation Plant and Nominal model:* The nominal model is shown as Fig. 4 and its parameter is shown in (I). The simulation plant has parametric modeling error: $J = 0.8J_n$ and $D = 1.2D_n$.

The rolling friction model used in the simulations is shown in Fig. 5. The width of region 1 showing nonlinear elastic characteristic is about $10\,\mathrm{\mu m}$ and Coulomb friction $T_c$ is $3.2\,\mathrm{N\,m}$.

*2) Design of Feedback Controller:* Feedback controller $C_{\mathrm{FB}}$ is a PID controller designed to have $30\,\mathrm{Hz}$ closed loop multiple poles by the pole placement method. It is discretized by the Tustin transformation with sampling time $T_s$.

*3) Design of Learning Filter and Robust Filter:* Learning filter $L(z)$ is designed as zero-phase tracking error controller [13] of $S_nP_n$. In addition, robust filter $Q(z)$ is $N_Q$th-order zero-phase low-pass filter.

$$Q(z) = \left(\frac{z + 2 + z^{-1}}{4}\right)^{N_Q}. \tag{24}$$

$Q(z)$ is non-causal and to realize $Q(z)$, $Q_r(z)$ with $N_Q$ samples delay compensation of the memory is implemented.

$$Q_r(z) = Q(z) \cdot z^{-N_Q}. \tag{25}$$

To satisfy ILC's monotonic convergence condition (7), $N_Q$ is set to be 16.

*4) Position Reference Trajectories and Basis Functions:* To verify robustness to reference trajectory variation, two types of position reference trajectories are used. First, "Ref. 1" in Fig. 9a is used and learned until the 5th trial. From the 6th trial, the reference trajectory is changed from "Ref. 1" to "Ref. 2". From the position references shown in Fig. 9a, each basis function is obtained as Fig. 9b–9d. Here, the tuning parameter $x_\mu$ is set to be $5\,\mathrm{\mu m}$.

*5) Design of Weighting Matrix:* The weighting matrix $\boldsymbol{W}_j$ is designed as

$$\boldsymbol{W}_j = \mathrm{diag}\begin{pmatrix} w_j[0] & w_j[1] & \cdots & w_j[N] \end{pmatrix}, \tag{26}$$

$$w_j[i] = \begin{cases} 1 & (x_{r,j}[i] > 100\,\mathrm{\mu m}) \\ 0 & (\text{otherwise}) \end{cases}, \tag{27}$$

where $x_{r,j}$ is displacement from stage's velocity reversal point. $x_{r,j}$ is calculated from position reference $r_j$. By introducing $\boldsymbol{W}_j$, the plant's parameters can be estimated from only information of the region where rolling friction shows Coulomb friction.

*6) Design of Data-based Friction Model:* The friction table for the data-based friction model is generated using information in the region where displacement from the stage's velocity reversal point is within $100\,\mathrm{\mu m}$. Then, feedforward input is calculated by using the data-based friction model. On the other hand, in the region where the displacement is over $100\,\mathrm{\mu m}$, the feedforward input is calculated by using estimated Coulomb friction.

### B. Results

The simulation results are shown in Fig. 10. Fig. 10a and 10b show Root-mean-square (RMS) and maximum (MAX) value of each trial's tracking error. These figures show that projection-based ILC can handle various reference trajectories, while standard ILC needs relearning after the reference trajectory is changed from "Ref. 1" to "Ref. 2". Fig. 10c and 10d show the tracking error of 1st trial after the reference trajectory variation. According to them, it can be said that tracking error decreases by using the data-based friction model.

The effectiveness of our proposal is verified by simulations.

## V. EXPERIMENT

Experiments are conducted under the same conditions as simulations. Experimental results are shown in Fig. 11 and show the same tendency as simulation. Experiments also verify the effectiveness of our proposal.

However, compared to standard ILC, projection-based ILC using basis functions and data-based friction model deteriorates a little after convergence. It can be thought that this deterioration is caused by unmodeled dynamics, disturbance, and noise.

## VI. CONCLUSION

ILC is a very effective tracking control method under the assumption that the same reference trajectory is repeated in each trial. However, once this assumption is violated, ILC cannot enhance control performance. To overcome this problem, studies on projection-based ILC have been conducted. In this paper, an application of projection-based ILC to position control of ball-screw-driven stages is considered. To suppress large tracking error caused by rolling friction, projection-based ILC using basis functions and data-based friction model is proposed. In this method, by estimating the plant's parameters and rolling friction in each trial, precise control can be achieved. The effectiveness of our proposal is verified through simulations and experiments. Verification in other situations (*e.g.* other reference trajectories) and proof of convergence of our proposal are future work.

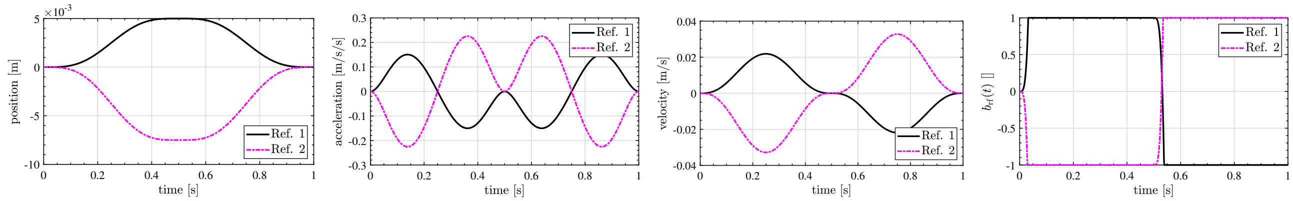


(a) Reference trajectories. (b) Acceleration. (c) Velocity. (d) $b_{\mathrm{rf}}(t)$ defined as (13).

Fig. 9: Position reference trajectories and basis functions. First, "Ref. 1" is used and then, "Ref. 2" is used from 6th trial.

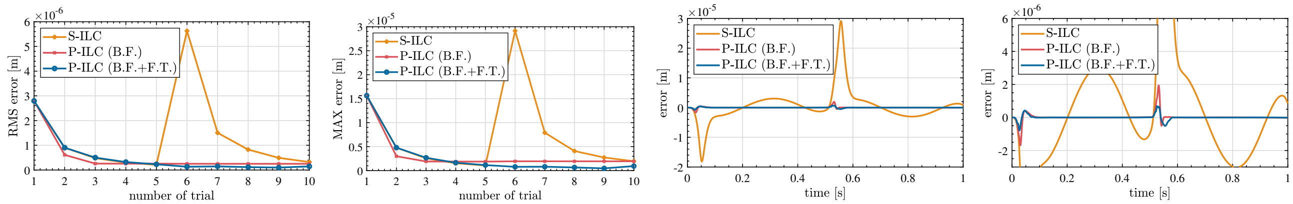


(a) RMS error of each trial. (b) Max error of each trial. (c) Tracking error of 6th trial. (d) Enlarged view of Fig. 10c.

Fig. 10: Simulation results.

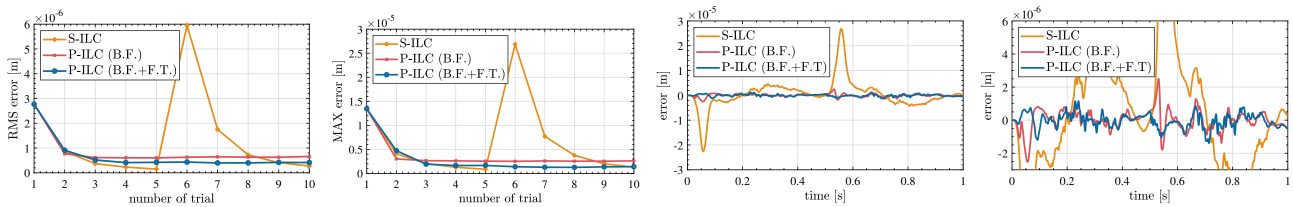


(a) RMS error of each trial. (b) Max error of each trial. (c) Tracking error of 6th trial. (d) Enlarged view of Fig. 11c.

Fig. 11: Experimental results.

## REFERENCES


[1] D. A. Bristow, M. Tharayil, and A. G. Alleyne, "A Survey of Iterative Learning Control," *IEEE Control Systems Magazine*, vol. 26, no. 3, pp. 96–114, 2006.

[2] T. Oomen, "Advanced Motion Control for Precision Mechatronics: Control, Identification, and Learning of Complex Systems," *IEEJ Journal of Industry Applications*, vol. 7, no. 2, pp. 127–140, 2018.

[3] F. Boeren, A. Bareja, T. Kok, and T. Oomen, "Frequency-Domain ILC Approach for Repeating and Varying Tasks: With Application to Semiconductor Bonding Equipment," *IEEE/ASME Transactions on Mechatronics*, vol. 21, no. 6, pp. 2716–2727, 2016.

[4] J. van Zundert, J. Bolder, and T. Oomen, "Optimality and flexibility in Iterative Learning Control for varying tasks," *Automatica*, vol. 67, pp. 295–302, 2016.

[5] F. Al-Bender, V. Lampaert, and J. Swevers, "The Generalized Maxwell-Slip Model: A Novel Model for Friction Simulation and Compensation," *IEEE Transactions on Automatic Control*, vol. 50, no. 11, pp. 1883–1887, 2005.

[6] Y. Maeda and M. Iwasaki, "Feedforward Friction Compensation Using the Rolling Friction Model for Micrometer-stroke Point-to-point Positioning Motion," *IEEJ Journal of Industry Applications*, vol. 7, no. 2, pp. 141–149, 2018.

[7] H. Asaumi and H. Fujimoto, "Proposal on nonlinear friction compensation based on variable natural length spring model," in *SICE Annual Conference*, 2008, pp. 2393–2398.

[8] T. Beauduin and H. Fujimoto, "Distributed and Parameter-Varying Friction Compensation for Ball-Screw Feed Drive Systems," in *The 3rd IEEJ International Workshop on Sensing, Actuation, Motion Control, and Optimization*, 2017.

[9] H. Fujimoto and T. Takemura, "High-Precision Control of Ball-Screw-Driven Stage Based on Repetitive Control Using $n$-Times Learning Filter," *IEEE Transactions on Industrial Electronics*, vol. 61, no. 7, pp. 3694–3703, 2014.

[10] T. Hayashi, H. Fujimoto, Y. Isaoka, and Y. Terada, "Basic Study of Iterative Learning Control Using Basis Functions for Various Tasks of a Ball-screw-driven Stage," in *The 5th IEEJ International Workshop on Sensing, Actuation, Motion Control, and Optimization*, 2019.

[11] T. Takemura and H. Fujimoto, "Proposal of novel rolling friction compensation with data-based friction model for ball screw driven stage," in *IECON 2010 - 36th Annual Conference on IEEE Industrial Electronics Society*, vol. 1. IEEE, 2010, pp. 1932–1937.

[12] ——, "Simultaneous identification of linear parameters and nonlinear rolling friction for ball screw driven stage," in *IECON 2011 - 37th Annual Conference of the IEEE Industrial Electronics Society*. IEEE, 2011, pp. 3424–3429.

[13] M. Tomizuka, "Zero Phase Error Tracking Algorithm for Digital Control," *Journal of Dynamic Systems, Measurement, and Control*, vol. 109, no. 1, pp. 65–68, 1987.